

# Stand Alone Dual Axis Sun Tracking System and Charge Controller

Hamza Khan, Dr. Senthil Arumugam Muthukumaraswamy

**Abstract** – This paper explains the design of an efficient dual axis sun tracking system using a complex algorithm to calculate the azimuth and elevation angles of the sun across the sky based upon real time feedback. The algorithm function was written in C/C++ programming language and integrated along with multiple other functions which were required to operate the electromechanical structure. Detailed explanation of the analogue charge controller is also included. This paper highlights the significance of the self-sufficient system and provides analysis of the experiments conducted using the prototype model. Furthermore, the proposed prototype consists of an Arduino UNO microcontroller, real time clock module, motor drivers, stepper motors, nine volt solar panel, a lead acid brick battery and the charge controller as its main components. This system can be put to multiple uses in order to harvest maximum renewable energy from the sun as well as be used as educational material.

**Index Terms**– Solar tracker, dual axis solar tracker, sun tracker, sun tracking algorithm, sun positioning algorithm, Arduino, sun tracking mechanism, float charge controller, charge controller, analogue charge controller.

## I. INTRODUCTION

The world's energy demands could be comfortably satisfied due to the abundance of solar irradiation on Earth. On average, each square meter of land on Earth is exposed to enough sunlight to generate 1,700 kWh of energy per annum using currently available technology. The total solar energy that reaches the Earth's surface could meet existing global energy needs 10,000 times over "Banerji Das, Abhinav, 2015" - [1]. Therefore, sunlight is an enormous energy source that goes to waste and harnessing it is one of the major keys to solve the energy crisis. Every location is convenient to harness solar energy because sunlight is abundant worldwide. Solar power can be captured on an industrial scale and can also be used to harness energy in small gadgets and houses. Also, solar power is capable of providing off grid electrification which is a more economical solution for remote areas that acquire electricity through diesel generators. The electricity produced will be free of cost for the consumer except for operations and maintenance cost and setup cost. Never the less, the consumer would benefit in the long run.

Two techniques are used to track the sun, Active Tracking and Passive Tracking, and they are implemented in two types of designs; Single Axis Trackers and Dual Axis Trackers. The main properties to consider when choosing the perfect tracker

are its tracking accuracy, yield and tracking technique. Moreover, three commercially used PV systems exist: Direct coupled, Stand alone and grid connected PV systems and this prototype is stand alone. Stand-alone PV system independently produces electricity and is best for remote locations far from electricity distribution. Battery banks are typically used for storage and the load is not connected directly. The battery provides stabilized voltage and current by cancelling out transients, provides high current to motors when required and stores excess energy to be used later. The proposed system is powered by a 12V, 1.2 Ah lead acid battery which is charged by the solar panel, thus being completely self-sufficient.

The tracking mechanism uses a sun positioning algorithm to keep the photovoltaic panel perpendicular to the sun at all times. It is important to mathematically calculate the position of the sun for any solar energy harnessing system which is looking for maximum efficiency. This can be achieved calculating the vector altitude of the sun and the azimuth angles as explained in "Duffie and Beckman" – [2]. The altitude of the sun is the angle between the acting line of the sun and the horizontal plane, this angle varies throughout the day. As per "Solar Power Generation" by Yokogawa - [3], this angle is 90° when the sun is directly overhead during solar noon and 0° when the sun is setting. Furthermore, the angular displacement from the north of the projection beam radiation on the horizontal axis is the solar azimuth. At solar noon, the sun is directly north in the southern hemisphere and it is directly south in the northern side of Earth. At any instant of time, the coordinates of the location of the sun and its trajectory path through the day can be determined from a mathematical framework. This leads to introduce the sun vector. It is an imaginary arrow running from the solar tracking mechanism directly to the centre of the sun. The sun path and the sun vector are the most crucial for steering the tracking mechanism to face the sun continuously.

With the solar positioning algorithm, the position of the sun in the sky is expressed as sun vectors, denoted in terms of elevation and azimuth angle of the sun, as mentioned on "Powerfromthesun.net" by Stine and Geyer – [4]. This algorithm is formulated to take the GPS coordinates of the tracker location and the date and time as inputs to determine the solar altitude and azimuth angle as the output for the particular geographical location. And, it takes the daily and seasonal solar path into consideration using astronomical principals.

On the other hand, the aim of the charge controller was to be capable of over voltage cut-off and over current cutoff with a convenient cut-in voltage. Hence, an analogue charge controller was designed using a five pin relay switch to perform the cut-off at 13V and a potentiometer to control the cut-offs to a certain degree.

**Hamza Khan**, Department of Engineering and Physical Sciences, Heriot-Watt University Dubai Campus, Dubai, United Arab Emirates, +971567477196.

**Senthil Arumugam**, Department of Engineering and Physical Sciences, Heriot-Watt University Dubai Campus, Dubai, United Arab Emirates.

## II. METHODOLOGY

The system starts by automatically calibrating itself with the help of two limit switches and always return the solar panel to its home position before starting to track the sun which was towards the North of the azimuth. This is followed by the sun position calculation which guides the two stepper motors towards the sun to maximize the energy harnessed by the photovoltaic module. The solar panel is connected to a charge controller that cuts off voltages higher than 13.3V and cuts back in at 12.9V, which is ideal to charge a 12V battery. The battery powers the microcontroller after the voltage is passed through a 5V regulator (Arduino input limit). The schematic block diagram of the sun tracking system is shown in Fig. 1.

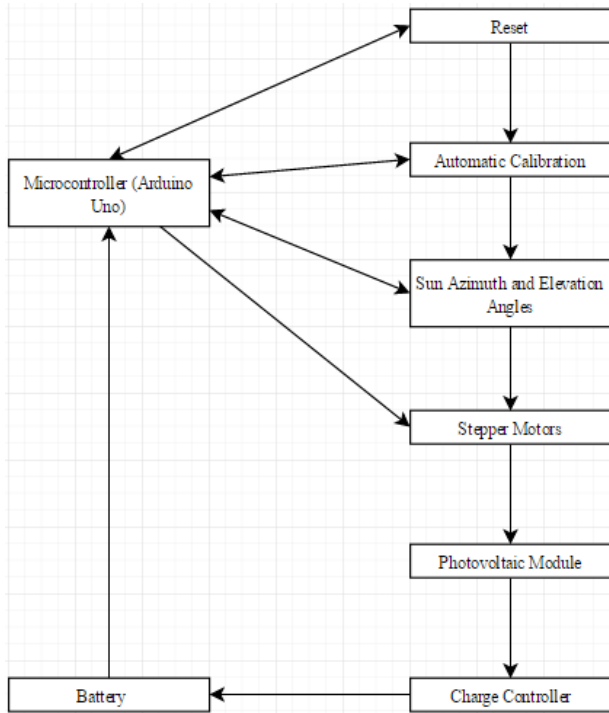


Fig. 1: Block schematic of the system operation.

### A. Microcontroller (Arduino Uno)

The microcontroller is the most crucial part of the system. An AVR, ATmega328 chip is the microcontroller that is mounted on the Arduino. The ATmega328 is an 8 bit AVR RISC based microcontroller that combines 32KB In System Programming flash memory, 1KB EEPROM, 2KB SRAM, 23 input/output general purpose registers, 3 compare mode enabled counters, external and internal interrupts, serial programmable USART, a 2 wire serial interface that is byte oriented, SPI serial port 10 bit analogue to digital converter, internal programmable oscillator and five power saving modes as described in “MegaAVR Microcontrollers” – [5]. It is connected to a real time clock module for real time feedback for sun positioning calculation and two motor drivers to operate the stepper motors that mount the solar panel. A program was written consisting of three main functions, one for keeping track of time which was most crucial for sun calculation, second to track the azimuth and elevation angles of the sun across the sky from 6am to 6pm (mean sunrise and sunset times in the UAE) using a complex algorithm and third for stepper motors to direct the solar panel in the direction guided by the algorithm. Motor1 tracks the azimuth angle and is connected to digital pins 8 to 11 on the

Arduino Uno and motor2 tracks the zenith/elevation angle and is connected to digital pins 4 to 7. The functions were then integrated together and compiled by the built in 32 – bit Arduino compiler.

### B. Sun Position Algorithm – Sun Azimuth and Elevation Angles

The sun location algorithm was written in a series of interlinked formulae that were used to derive the azimuth and elevation angles of the sun with respect to the horizon of the tracking mechanism. The algorithm was started by printing the latitude and longitude values on the status monitor display followed by converting the longitudinal distance from the sun to tracker to tracker to sun. Moreover, the ‘hour1’ value from the RTC was added to four to set the time difference between Greenwich and UAE.

Furthermore, the ‘JD\_Whole’ value which was defined as a date in the Julian calendar including year, month and day and a Julian date fraction was also calculated (Fig. 2) for which the value of ‘minute1’ from the RTC was subtracted by forty to match the difference between Julian time and real time, both of ‘JD\_Whole’ and ‘JD\_frac’ would assist in calculating the Julian day in the algorithm. Moreover, the minutes and hour formats were also set using ‘if’ statements and forty was added back to ‘minute1’ after the Julian date fraction calculation which is shown in Fig. 3b.

```

long JulianDate(int year1, int month1, int day1)
{
    long JD_whole;
    int A,B;
    if (month1<=2)
    {
        year1--;
        month1+=12;
    }
    A=year1/100;
    B=2-A+A/4;
    JD_whole=(long) (365.25*(year1+4716))+(int) (30.6001*(month1+1))+day1+B-1524;
    return JD_whole;
}
    
```

Fig. 2: Julian date calculation.

Then, the derivation of elevation and azimuth angles was commenced by calculating the Julian day and Julian century with respect to beginning of the twentieth century. This was followed by the geometric mean longitude of the sun in radians and the geometric mean anomaly of the sun for the angular distance travelled. The eccentric Earth orbit was then calculated by using the integers of Julian century followed by the sun’s equation of center in radians using the mean anomaly and Julian century values and after that the sun true longitude was calculated by adding the mean longitude with previously calculated value of equation of center. These would help determine the longitude from the center of the sun.

Furthermore, the mean oblique elliptical angle of the sun was calculated and converted to radians followed by the hour angle calculations which were also converted to radians. The distance from the tracker to the centre of the sun was then found including the angle it made with the normal of the tracking mechanism. After that, the sun declination angle was calculated through the assistance of mean oblique and true longitude values and this led to the derivation of solar elevation and azimuth.

Using the hour angle, latitude value in radians and sun declination angle, the two values of solar azimuth and elevation were derived and converted back to degrees and the direction of the imaginary vector arrow to the centre of the sun was changed back to facing the tracker from the sun. The complete derivation process is showed in Fig. 3c.

```
void sun_position_calculation()
{
  Serial.print("Longitude and latitude ");
  Serial.print(Lon/DEG_TO_RAD,3);
  Serial.print(" "); Serial.println(Lat/DEG_TO_RAD,3);
  Serial.println("year1,month1,day1,local hour1,minutel,second1,elevation,azimuth");
  Lon=0-Lon; //changing the longitudinal distance from sun to tracker to tracker to sun
  hour1 += 4; //adding time difference from GMT
}
```

Fig. 3a: Printing longitude and latitude values, inverting the longitudinal distance from the sun and adding time difference.

```
JD_whole=JulianDate(year1,month1,day1);
minutel -= 40;
if(minutel < 0)
{
  hour1--;
  minutel = 60 + minutel;
}
JD_frac=(hour1+minutel/60.+second1/3600.)/24.-.5;

minutel += 40;
if(minutel >= 60)
{
  hour1 += 1;
  minutel = minutel-60;
}

if(JD_frac < 0)
{
  JD_whole -=1;
  JD_frac = 1 + JD_frac;
}
```

Fig. 3b: Defining the Julian date and Julian date fraction setting the format of time.

```
T=JD_whole-2451545; T=(T+JD_frac)/36525.;
LO=DEG_TO_RAD*fmod(280.46645+36000.76983*T,360);
M=DEG_TO_RAD*fmod(357.5291+35899.0503*T,360);
e=0.016708617-0.000042037*T;
C=DEG_TO_RAD*((1.9146-0.004847*T)*sin(M)+(0.019993-0.000101*T)*sin(2*M)+0.00029*sin(3*M));
f=M+C;
Ob1=DEG_TO_RAD*(23+26/60.+21.448/3600.-46.815/3600*T);
JDx=JD_whole-2451545;
GrHrAngle=280.46061837+(360*JDx)/360+98564736629*JDx+360.98564736629*JD_frac;
GrHrAngle=fmod(GrHrAngle,360.);
L_true=fmod(C+LO, TWOPI);
R=1.000001018*(1-e*e)/(1+e*cos(E));
PA=atan2(sin(L_true)*cos(Ob1),cos(L_true));
Decl=asin(sin(Ob1)*sin(L_true));
HrAngle=DEG_TO_RAD*GrHrAngle+Lon-PA;
elev=asin(sin(Lat)*sin(Decl)+cos(Lat)*cos(Decl)*cos(HrAngle));
// Azimuth measured eastward from north.
azimuth=PI+atan2(sin(HrAngle),cos(HrAngle)*sin(Lat)-tan(Decl)*cos(Lat));
azimuth_angle = azimuth/DEG_TO_RAD;
elevation_angle = elev/DEG_TO_RAD,2;
Lon=0-Lon;
```

Fig. 3c: Deriving solar azimuth and elevation and converting them to degrees, also resetting the longitudinal distance.

The sun position calculation in the figures above was followed by printing the essential variables on the Arduino serial monitor for the observer.

### C. Stepper Motors

The two stepper motors are controlled via their motor drivers which receive impulses from the microcontroller as per the calculated sun angle. The motors' function is to set the solar panel to home position and then respond to the calculated angles and always keep the panel perpendicular to the sun.

The unregulated voltage from the 9V solar panel goes to four 4.6Ω parallel resistors that make a total resistance of 1.15Ω with a total wattage of 1W, hence it dissipates no more than 1W. Parallel resistor connection was assembled due to the lack of 1Ω, 1W resistors. Fig. 4 shows the connections flowchart of the stand alone system.

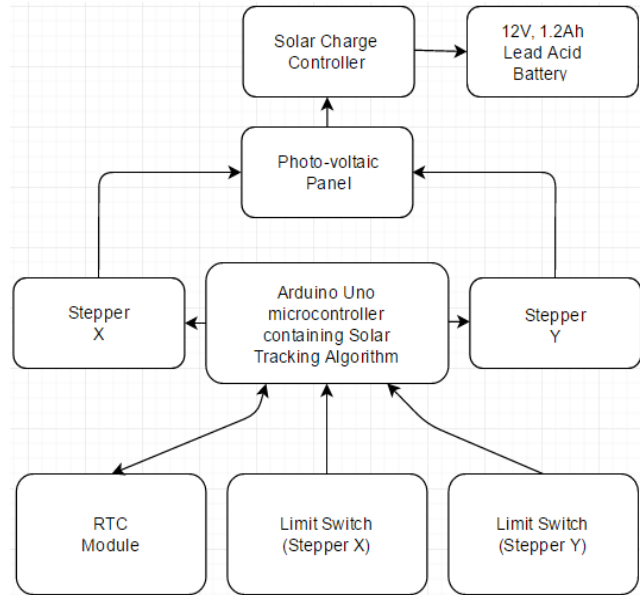


Fig. 4: Overview of the system connections.

### D. Photovoltaic Cells

The three main types of photovoltaic cells are:

- Monocrystalline
- Polycrystalline
- Thin film

However, other relevant technologies include organic PV cells and multi-junction PV panels are quickly making their statement too. Monocrystalline cells are made of a single rigid silicon crystal. They are not cheap to produce but 10 – 14% efficient with a smooth and thick texture - [1]. Polycrystalline cells are cut out of a block of silicon consisting of several crystals. They have a shiny, reflective surface but are also lesser efficient - [1]. Thin film cells are produced from non-crystalline silicon or other materials such as copper selenide or cadmium telluride. They are flexible and 5 – 8% efficient. They offer good low light performance hence are less affected by shading as mentioned in “Solar PV Panels” - [6]. Moreover, Multi-junction cells contain different materials and can achieve efficiencies over 40% which is twice the normal PV cell output. However, they are comparatively expensive - [7]. The cheapest solar cells are organic cells, made of organic material. They are not yet used for residential systems because of the very low efficiency - [8]. Therefore, a 9V monocrystalline cell was installed to harness solar energy because it had the best average performance outdoors.

### E. Analogue Charge Controller

However, this resistance limits the incoming current and drops the voltage by 0.13V as per testing. The current then reaches the middle (main) pin of the relay - which is connected to the normally closed switch of the relay, and also branches to provide magnetizing current to one connection of the relay coil. This pin from the normally closed switch is

connected directly to the battery and the relay allows charging until the magnetizing current is reached. The second relay coil is connected with an NPN transistor emitter and the base is linked with a 10kΩ potentiometer which can control the relay cut-off voltage to a certain degree by varying the line resistance. The schematic of the charge controller is shown below in Fig. 5.

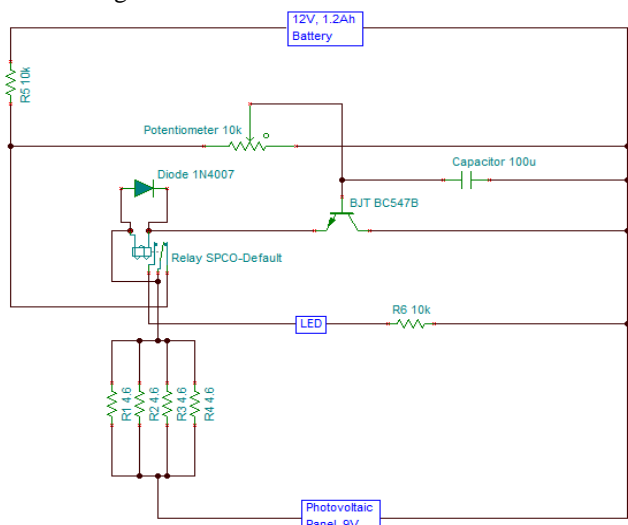


Fig. 5: Circuit schematic of the analogue charge controller.

Furthermore, a 100µF, 25V capacitor is also connected in parallel with the transistor to filter the irregular DC voltage and sudden voltage spikes to keep the circuit safe and efficient. The relay coil is kept segregated by connecting a forward bias diode between both relay coil connections to terminate any chances of a short circuit. On the other hand, the normally open switch of the relay is connected with an LED to the negative line and a 3kΩ resistor to avoid damaging the LED. When the relay coil magnetizing threshold is reached the normally open switch closes and the LED indicates voltage cut-off. The negative of the circuit is kept common among all the components.

Upon testing it is observed in Fig. 6a that the relay coil is magnetized at a 13.3V input from the power supply. Moreover, a voltage drop of 0.4V is needed to demagnetize the relay coil which can be observed in Fig. 6b, hence the cut-in voltage is 12.9V.

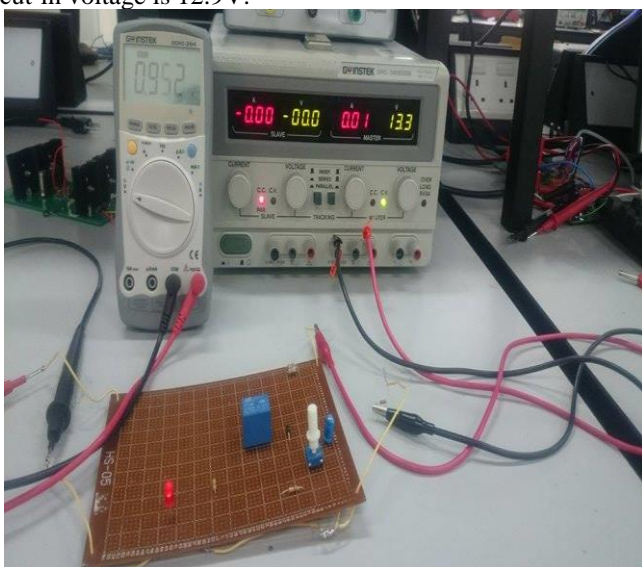


Fig. 6a: At 13.3V from the power supply, the relay cuts off the circuit.

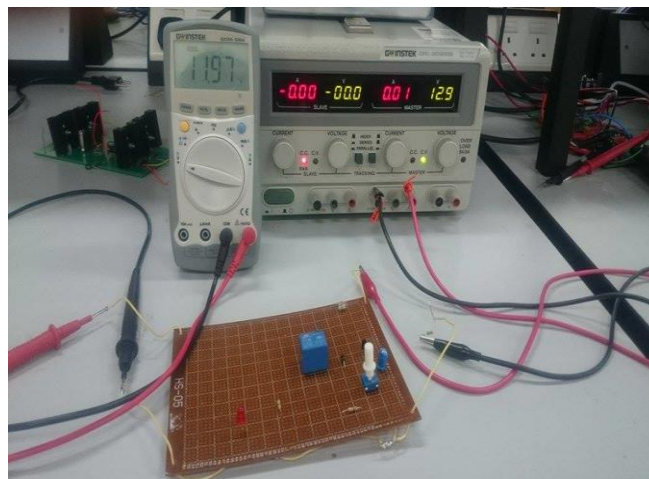


Fig. 6b: At an input of 12.9V the relay coil is demagnetized and cut-in voltage is determined to be 12.9V.

### III. EXPERIMENTAL RESULTS

A series of experiments were conducted with the charge controller and the tracking mechanism. Each value related to measuring was measured thrice during experimentation and the average was used to keep the experimental standard high and obtain precise results. Furthermore, sun tracking was conducted over a three days period and the readings from status monitor and solar panel outputs were recorded on frequent intervals and analyzed.

#### A. Charge Controller

The experiments conducted with the charge controller included controller output (Fig. 7), voltage drops, cut-off voltage, cut-in voltage and oscilloscope waveform and reading. The aim of the experiments was to measure and ensure good efficiency and performance of the controller.

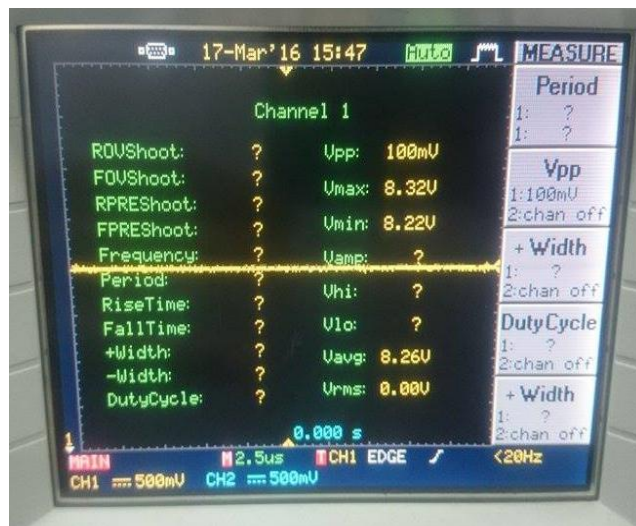


Fig. 7: DC voltage waveform of the controller output.

The figure above shows the DC voltage waveform of the charge controller output after a 9V input voltage was applied through the supply because the solar panel used in the prototype was 9V. However, it was observed the maximum and minimum voltages were 8.32V and 8.22V respectively, resulting in an average voltage of 8.26V, hence a mean voltage drop of 0.74V. The peak to peak voltage was minimal because of the waveform not being sinusoidal. Table 1 portrays the experiment results.

Table 1: Charge controller output.

Supply Voltage (V)	Controller Output (V)	Desired Output (V)
4.00	3.31	4.00
6.00	5.23	6.00
8.00	7.17	8.00
10.0	9.12	10.0
12.0	11.14	12.0

Mean Voltage Drop can be calculated as

$$\frac{(0.69+0.77+0.83+0.88+0.6)}{5} = 0.754V.$$

This voltage drop was mainly due to threshold voltage of the two 1n4007 diodes that were used and the 25V capacitor. Therefore, the mean controller output at 9V supply was 8.25V (9 – 0.754). Hence,

The Controller Efficiency at 9V =  $\frac{8.25}{9} \times 100 = 91\%$  which is excellent and proves that the controller was efficient.

### B. Sun Elevation and Azimuth Angles

The tracking mechanism was tested over three days and the values observed in the serial monitor were plotted in Figures 8 – 10 for further analysis.

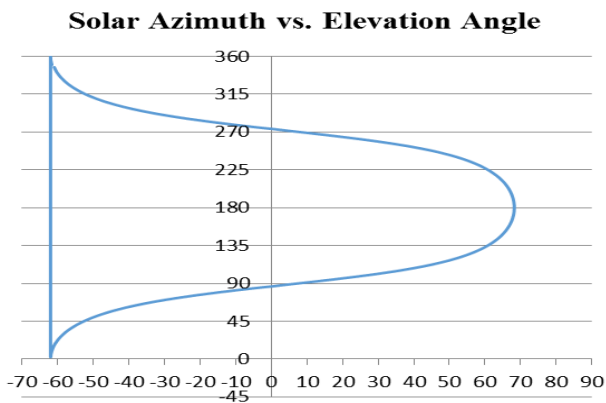


Fig. 8a: Solar azimuth vs elevation angles throughout the day 1.

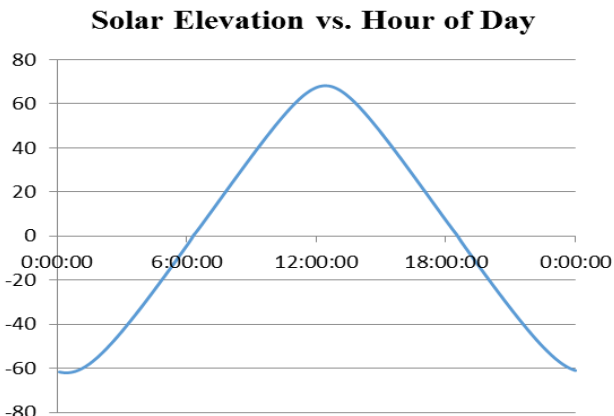


Fig. 8b: Elevation of the sun recorded through the day 1 calculated by disabling the boundary conditions.

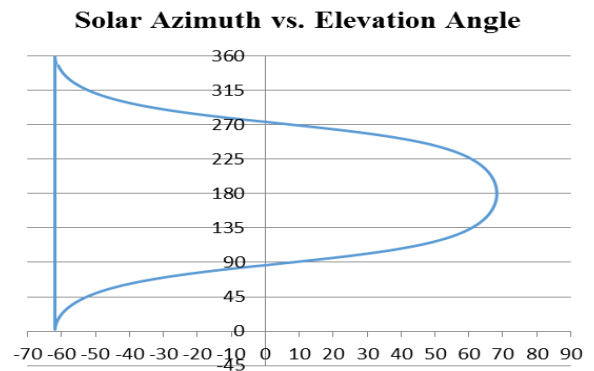


Fig. 9a: Solar azimuth vs elevation angles throughout the day 2.

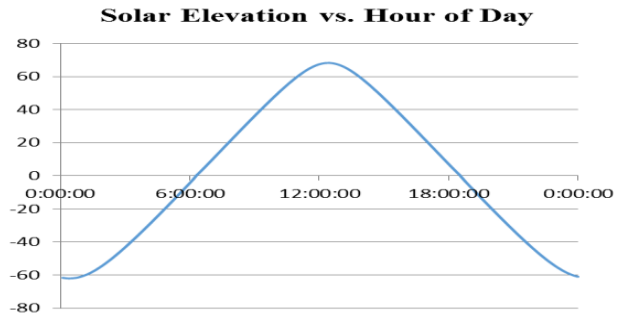


Fig. 9b: Elevation of the sun recorded through the day 2 calculated by disabling the boundary conditions.

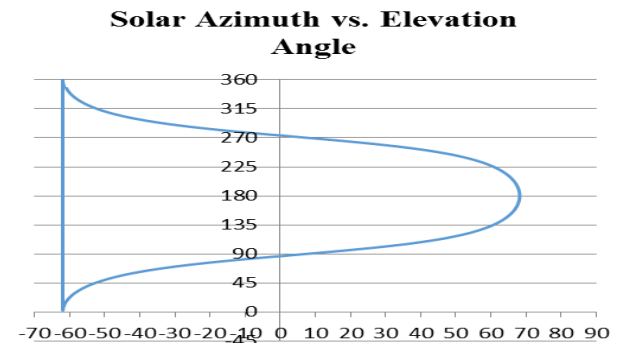


Fig. 10a: Solar azimuth vs elevation angles throughout the day 3.

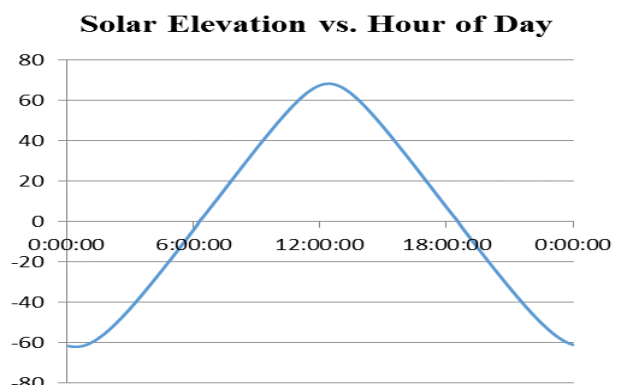


Figure 10b: Elevation of the sun recorded through the day 3 calculated by disabling the boundary conditions.

From the figures 8 – 10, it was observed that the azimuth and elevation angles over the three days changed narrowly during the middle of the day and the sunrise time was slightly different. The diurnal circles followed by the sun over the three day course could also be visualized through the graphs.

C. Solar Panel Output Voltage

The output voltage from the 9V solar panel on the tracker was also recorded at an hourly interval over the three days and compared to a similar 9V solar panel output that was fixed at 45° East. Also, the panels were kept clean of dust and dirt to assure maximum output. From figures 11 a – c, the outcome of the experiment was analyzed on a daily basis.

- Day 1 – Clear day but partly cloudy before sunset.

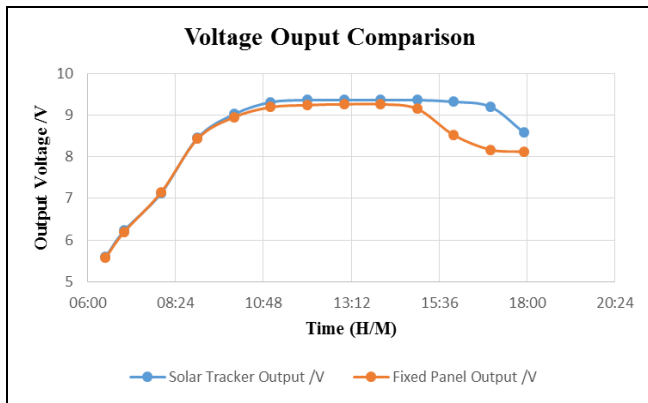


Fig. 11a: Output voltage comparison on day 1.

- Day 2 – Humid and cloudy weather until afternoon.

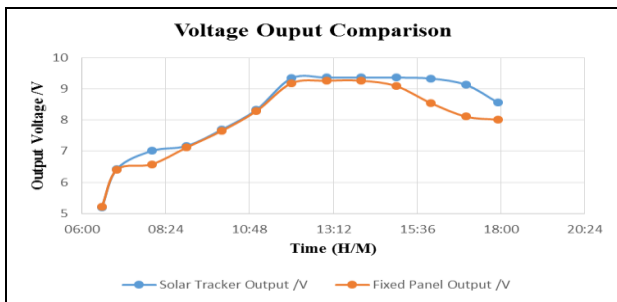


Fig. 11b: Output voltage comparison on day 2.

- Day 3 – Clear day

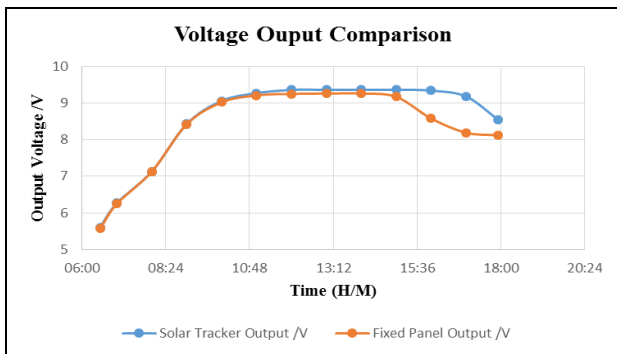


Fig. 11c: Output voltage comparison on day 3.

The maximum output of both panels was recorded as 9.36V and 9.26V for the solar panel on tracker and the fixed panel respectively. Although the panels used were of similar specifications, the maximum output capability was observed to be different.

On day one the efficiency from the solar tracker is

$$\text{efficiency} = \frac{\text{Mean Output}}{\text{Maximum Output}} \times 100 = \frac{8.48}{9.36} \times 100 = 90.6\%$$

The fixed panel efficiency is

$$\text{efficiency} = \frac{\text{Mean Output}}{\text{Maximum Output}} \times 100 = \frac{8.24}{9.26} \times 100 = 88.98 \approx 89.0\%$$

Furthermore, the tracker efficiencies on days 2 and 3 were 87.3% and 90.6% respectively and the fixed panel efficiencies were 85.3% and 89.2% respectively.

IV. STAND ALONE SYSTEM

The previously done experiments proved that each department of the prototype model was performing efficiently and they could all be combined to make a DC coupled system. Therefore, the photovoltaic panel was connected with the charge controller which was then connected to the 12V, 1.2Ah battery. The system was able to charge the fully drained battery up to 9.33V due to the panel output limitations, hence the potential difference couldn't get higher. It took 3 hours and 24 minutes to charge which is equal to 3.4 hours, therefore the mean current drawn by the battery can be  $\frac{1.2}{4.2} = 0.29A$ . Thus the mean power output of the solar panel was  $P = VI = 9.04 \times 0.29 = 2.62W$ . This leads to derive the tracking system efficiency over the fixed panel efficiency in terms of power.

$$\text{Efficiency} = \frac{\text{power output difference}}{\text{tracking system power output}} \times 100 = \frac{3.26 - 2.62}{3.26} \times 100 = 19.6\%$$

The tracking system power output is 19.6% more efficient as compared to the fixed panel system. However, it should be noted that the two systems charged the battery on two separate days because only one charge controller and battery were available each.

V. CONCLUSION

The proposed system proved to be 19.6% more efficient compared to the fixed panel system over a three day period while harnessing maximum solar power as per its capability. Furthermore, the lead acid battery was successfully charged and the charge controller was working efficiently and possessed over voltage and over current cut-off facility. However, a larger experimentation time frame would drastically increase the system efficiency. The prototype model could be taken forward as a reference tracker for manual tracking installations, this would be a cheap and efficient method to harness maximum solar energy. Moreover, the proposed system could also be adopted for educational purposes.

ACKNOWLEDGMENT

By the grace of the Almighty God, worthy of all praises, and due to His uncountable blessings I was able to complete

the sun tracking system successfully. I am grateful towards my parents and would also like to offer my profound gratitude towards Dr. Senthil Arumugam Muthukumaraswamy, for his guidance and healthy criticism. Furthermore, I acknowledge the Heriot Watt University for providing me good exposure in the educational field of Electrical and Electronics and providing any available materials required for the prototype completion.

#### REFERENCES

- [1] Banerji Das, Abhinav. "A Guide to Solar Power Generation In The United Arab Emirates". Web address: <http://www.mesia.com/wp-content/uploads/Solar%20for%20Students.pdf> . Retrieved, 27/11/15.
- [2] Duffie, J.A. and Beckman, W.A. (2006). "Solar Engineering of Thermal Processes". 3rd edn. Wiley. ISBN 047169867
- [3] Yokogawa (2014). "Solar Power Generation" - Features of the HXS10 SolStation "Solar Tracking Control: Built-In Solar Position Algorithm". Yokogawa Electric Corporation, Solar Power Generation - "Making Use of Solar Energy" - Volume 1, no. 1-8. Web address: <http://www.yokogawa.com/> . Retrieved, 04/01/2016.
- [4] Stine, W.B. and Geyer, M. (2001). "Powerfromthesun.Net". Web address: <http://powerfromthesun.net/> . Retrieved, 12/1/2016.
- [5] "MegaAVR Microcontrollers". Web address: <http://Atmel.com/> . Retrieved 21/01/16.
- [6] "Solar PV Panels", Web address: <https://www.solarguide.co.uk/> . Retrieved, 5/12/2015.
- [7] "Multi Junction Solar Cells". Web address: <http://reuk.co.uk/> . Retrieved, 8/12/2015.
- [8] Research: Next-Generation Photovoltaic Technologies. Web address: <http://www.anl.gov/> . Retrieved, 22/12/2015.



**Hamza Khan** completed his B.Eng (Hons.) in Electrical and Electronics Engineering from Heriot-Watt University Dubai Campus in 2016. His Honours thesis consisted of research and development of a sun tracking system prototype. His proposal on solar energy generating and harnessing system was nominated and selected at a solar integration competition and the idea was implemented at a rural franchise. His research

interests are in the field of renewable energy generation and solution, and smart grids.



**Senthil Arumugam Muthukumaraswamy** is presently working as an Asst. Professor in School of Engineering and Physical sciences, Heriot-Watt University Dubai campus since 2009. Prior to this, he was working in Malaysia and India, for about 14 years. He obtained his BE degree in 1994 from Madras University, India and M.S (Engg) in 1998

from BITS, Pilani, India and Ph.D (Engg) in 2008 from Multimedia University, Malaysia. He has also obtained the Post Graduate Certificate in Academic process (PGCAP) from Heriot-watt University in 2011 and thus became the fellow of higher education academy (FHEA). His research interests are Optimization algorithms, soft computing, digital signal processing, etc. He has published more than 35 international publications.